J|A|C|S
ARTICLES
Published on Web 10/05/2007

TROSY-Based *z*-Exchange Spectroscopy: Application to the Determination of the Activation Energy for Intermolecular Protein Translocation between Specific Sites on Different DNA Molecules

Debashish Sahu,[†] G. Marius Clore,[‡] and Junji Iwahara*[,†]

Contribution from the Department of Biochemistry and Molecular Biology and Sealy Center for Structural Biology and Molecular Biophysics, University of Texas Medical Branch, Galveston, Texas 77555-0647, and Laboratory of Chemical Physics, National Institute of Diabetes and Digestive and Kidney Disease, National Institutes of Health, Bethesda, Maryland 20892-0520

Received June 22, 2007; E-mail: j.iwahara@utmb.edu

Abstract: A two-dimensional TROSY-based *z*-exchange $^{1}H-^{15}N$ correlation experiment for the quantitative analysis of kinetic processes in the slow exchange regime is presented. The pulse scheme converts the product operator terms N_z into $2N_zH_z$ and $2N_zH_z$ into $-N_z$ in the middle of the *z*-mixing period, thereby suppressing the buildup of spurious semi-TROSY peaks arising from the different relaxation rates for the N_z and $2N_zH_z$ terms and simplifying the behavior of longitudinal magnetization for an exchanging system during the mixing period. Theoretical considerations and experimental data demonstrate that the TROSY-based *z*-exchange experiment permits quantitative determination of rate constants using the same procedure as that for the conventional non-TROSY $^{15}N_z$-exchange experiment. Line narrowing as a consequence of the use of the TROSY principle makes the method particularly suitable for kinetic studies at low temperature, thereby permitting activation energies to be extracted from data acquired over a wider temperature range. We applied this method to the investigation of the process whereby the HoxD9 homeodomain translocates between specific target sites on different DNA molecules via a direct transfer mechanism without going through the intermediary of free protein. The activation enthalpy for intermolecular translocation was determined to be 17 kcal/mol.

Introduction

NMR exchange spectroscopy (EXSY) is a powerful tool for studying dynamic processes in the slow exchange regime. The methodology permits the determination of rate constants for both forward and backward reactions at equilibrium. Two-dimensional $^{1}H-^{1}H$ EXSY experiments, first proposed by Jeener et al. in 1979,[1] have been extensively used for kinetic investigations of various chemical exchange processes involving small organic compounds (see ref 2 for a review). For macromolecules, $^{1}H-^{1}H$ EXSY experiments are generally less suited since exchange and NOE peaks are present and may be difficult to separate owing to extensive chemical shift overlap.[3] Exchange experiments involving heteronuclear longitudinal magnetization of product operator terms such as $2S_zI_z$ and S_z that only detect exchange processes were therefore proposed.[4,5] *z*-Exchange experiments based on heteronuclear correlation spectroscopy have been used for quantitative kinetic investigations of conformational exchange,[4a,6−9] protein/RNA folding,[4b,5,10] and protein−ligand interactions.[11−13]

In principle, activation energies can be obtained from the temperature dependence of the measured rate constants. For biological macromolecules, the available temperature range is limited owing to sample instability at high temperature and poorer quality spectra (i.e., extensive line broadening) at low temperature owing to longer rotational correlation times. In this paper, we demonstrate the utility of a $^{1}H-^{15}N$ TROSY-based *z*-exchange experiment for quantitative determination of rate constants, which is suitable for both low temperature measurements and large molecular weight systems. The extension of a $^{1}H-^{15}N$ TROSY-based pulse scheme to a *z*-exchange experi-

[†] University of Texas Medical Branch.
[‡] National Institutes of Health.

(1) Jeener, J.; Meier, B. H.; Bachmann, P.; Ernst, R. R. *J. Chem. Phys.* **1979**, *71*, 4546−4553.
(2) Perrin, C. L.; Dwyer, T. J. *Chem. Rev.* **1990**, *90*, 935−967.
(3) (a) Clore, G. M.; Driscoll, P. C.; Wingfield, P. T.; Gronenborn, A. M. *Biochemistry* **1990**, *29*, 7384−7401. (b) Clore, G. M.; Omichinski, J. G.; Gronenborn, A. M. *J. Am. Chem. Soc.* **1991**, *113*, 4350−4351.
(4) (a) Montelione, G. T.; Wagner, G. *J. Am. Chem. Soc.* **1989**, *111*, 3096−3098. (b) Wider, G.; Neri, D.; Wüthrich, K. *J. Biomol. NMR* **1991**, *1*, 93−98.
(5) Farrow, N. A.; Zhang, O.; Forman-Kay, J. D.; Kay, L. E. *J. Biomol. NMR* **1994**, *4*, 727−734.
(6) Otting, G.; Liepinsh, E.; Wüthrich, K. *Biochemistry* **1993**, *32*, 3571−3582.
(7) Nieto, P. M.; Birdsall, B.; Morgan, W. D.; Frenkiel, T. A.; Gargaro, A. R.; Feeney, J. *FEBS Lett.* **1997**, *405*, 16−20.
(8) Spranger, R.; Gribun, A.; Hwang, P. M.; Houry, W. A.; Kay, L. E. *Proc. Natl. Acad. Sci. U.S.A.* **2005**, *102*, 16678−16683.
(9) Bosco, D. A.; Eisenmesser, E. Z.; Pochapski, S.; Sundquist, W. I.; Kern, D. *Proc. Natl. Acad. Sci. U.S.A.* **2002**, *99*, 5247−5252.
(10) Wenter, P.; Bodenhausen, G.; Dittmer, J.; Pitsch, S. *J. Am. Chem. Soc.* **2006**, *128*, 7579−7587.
(11) Iwahara, J.; Clore, G. M. *J. Am. Chem. Soc.* **2006**, *128*, 404−405.
(12) John, M.; Headlam, M. J.; Dixon, N. E.; Otting, G. *J. Biomol. NMR* **2007**, *37*, 43−51.
(13) Cai, M.; Huang, Y.; Suh, J.-Y.; Louis, J. M.; Ghirlando, R.; Craigie, R.; Clore, G. M. *J. Biol. Chem.* **2007**, *282*, 14525−14535.

10.1021/ja074604f CCC: $37.00

ment is nontrivial since the simplistic incorporation of a *z*-mixing period following the t_1 evolution period results in undesired buildup of spurious peaks owing to different relaxation rates for the N_z and $2N_zH_z$ terms. We have solved this problem by incorporating a scheme to convert the N_z term into $2N_zH_z$ and the $2N_zH_z$ term into $-N_z$ in the middle of the *z*-mixing period. This scheme has the additional benefit of simplifying the behavior of the magnetizations of these two terms in an exchanging system, allowing one to determine rate constants from the dependence of the auto- and exchange-peak intensities as a function of mixing time in the same way as that for the conventional non-TROSY $^{15}N_z$-exchange experiment. Because of line narrowing arising from use of the TROSY principle,[14] the quality of data obtained with the new pulse sequence at low temperature is far superior to that for the conventional non-TROSY *z*-exchange experiment. The pulse sequence permits kinetic analysis over a wider range of temperature and is therefore suitable for the determination of activation energies for exchange processes involving biological macromolecules. The utility of the method is demonstrated by determining the activation energy for the translocation of the HoxD9 homeodomain from its specific target site on one DNA molecule to another. This exchange reaction involves direct transfer of the protein between DNA molecules without going through the intermediary of free protein and plays an important role in the target search process whereby a transcription factor locates its specific DNA target site.[11,15,16]

Materials and Methods

NMR Sample. The ^{2}H-/^{15}N-labeled HoxD9 homeodomain and double-stranded DNA duplexes (24 base pairs) were prepared as described previously.[11,14] The base sequence of one strand of DNA duplex *a* is 5′d-CACCTCT**C**TAATGGCTCACACCTG-3′ (with the homeodomain binding site underlined). The equivalent strand for DNA duplex *b* is identical except that the C·G base pair indicated in bold is replaced by an A·T base pair. The affinities of HoxD9 for DNA duplexes *a* and *b* DNA are virtually identical.[11] The NMR sample contained 0.7 mM ^{2}H-/^{15}N-labeled protein, 0.4 mM DNA duplex *a*, and 0.6 mM DNA duplex *b* in a buffer comprising 10 mM sodium phosphate (pH 6.5), 40 mM NaCl, 0.4 mM NaF (as an antibacterial agent), and 93% H_2O/7% D_2O. Under these conditions, all the protein is bound to DNA (either duplex *a* or *b*) and the molar ratio of the two complexes *a* and *b* is 2:3. Although a Tris·HCl buffer was used for the previous investigation,[11] we used phosphate buffer for the present study since the pH of Tris·HCl is highly dependent on temperature.

NMR Spectroscopy. All NMR data were recorded on the Varian NMR system operated at a ^{1}H-frequency of 800 MHz. The TROSY-based *z*-exchange ^{1}H−^{15}N correlation experiments (Figure 1A) were carried out at 8, 15, 20, 30, and 35 °C. Data with eight different mixing times between 0.02 s and 0.65 s were acquired in an interleaved manner. Sixteen scans were accumulated per FID, and the maximum values of t_1 and t_2 were 67 and 54 ms, respectively, yielding a measurement time of about 23 h. All other details of the NMR experiment are described in the caption to Figure 1. For comparison, $^{15}N_z$-exchange ^{1}H−^{15}N correlation spectra[5] were collected at 8 and 20 °C using the same number of scans, data points, and spectral widths as those used for the TROSY-based *z*-exchange experiment. NMR data were processed using NMRPipe,[17] and the spectra were analyzed using NMRView.[18] The rate constants were obtained by best-fitting the intensities of auto- and exchange peaks as a function of mixing time by numerically integrating the McConnell equations (cf. eq 9) and optimizing the unknown parameters (rate constants, spin-latice relaxation rate and scale factors) using the program FACSIMILE[19] as described previously.[3,11]

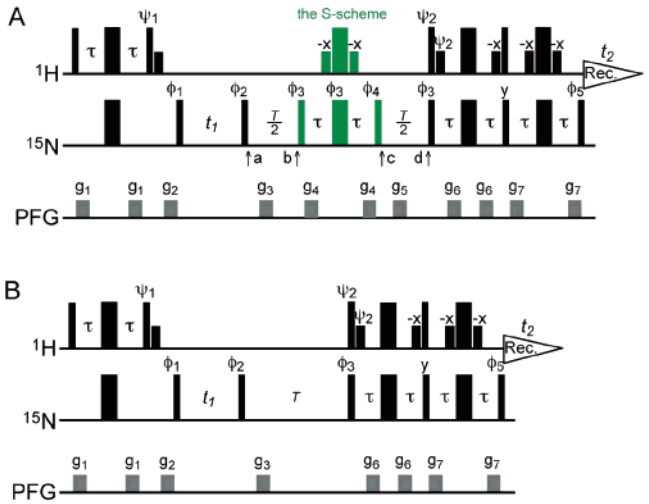

Figure 1. Pulse sequences for TROSY-based *z*-exchange spectroscopy. (A) Pulse sequence for the TROSY-based *z*-exchange 2D ^{1}H−^{15}N correlation experiment incorporating the S-scheme to suppress the buildup of spurious semi-TROSY peaks during the mixing period. Thin and bold bars represent 90° and 180° pulses, respectively. Unless indicated otherwise, pulse phases are *x*. ^{1}H pulses represented by short bold bars are soft rectangular 90° pulses selective to water (1.2 ms). The delay τ is set to 2.7 ms. The S-scheme (colored in green) is applied in the middle of the *z*-mixing period *T* to convert N_z into $2H_zN_z$ and $2N_zH_z$ into $-N_z$ terms. For Varian spectrometers, the phase cycles are as follows: $\phi_1 = \{x, -x, y, -y\}$; $\psi_1 = -y$; $\phi_2 = \{2(x, -x, y, -y), 2(-x, x, -y, y)\}$; $\phi_3 = \{-x, x, -y, y\}$; $\phi_4 = \{y, -y, -x, x\}$; $\phi_5 = \{4x, 4(-x)\}$; $\psi_2 = \{4(-y), 4y\}$; rec. $= \{x, -x, y, -y, x, -x, -y, y, -x, x, -y, y, -x, x, y, -y\}$. For Bruker spectrometers, *y* and $-y$ should be swapped for the ψ_1 and receiver phases. The difference in phases required for the two spectrometer systems is due to the fact that the manner used to shift phase for positive and negative gyromagnetic nuclei is instrument dependent, as noted previously in the literature.[34−36] Quadrature detection in the t_1 domain was achieved using States-TPPI, incrementing the phase ϕ_1. Amplitudes and lengths of pulse field-gradients were as follows: g_1, 8 G/cm, 1.0 ms; g_2, −19 G/cm, 1.7 ms; g_3, −19 G/cm, 1.0 ms; g_4, 8 G/cm, 0.6 ms; g_5, 12 G/cm, 0.7 ms; g_6, 12 G/cm, 0.6 ms; g_7, 15 G/cm, 0.7 ms. The rate constants for exchange were determined from the intensities of the exchange- and auto-peaks recorded in a series of 2D spectra with different values of *T*. (B) Simplistic version of a TROSY-based z-exchange experiment without incorporation of the S-scheme. Phase ψ_2 is $\{4(y), 4(-y)\}$ for the TROSY selection; other phases are as those in (A). The pulse sequence of panel B was used for Figure 2C but in practice is not suitable for quantitative applications (see text). For each pulse sequence, the consequences of the phase cycles employed were analyzed with the program POMA[37] for both ^1H_z- and $^{15}N_z$-derived magnetizations.

Theoretical Considerations

First, we consider the behavior of the components of *z*-magnetization during the mixing period for a nonexchanging ^{15}N−^{1}H spin system. At point a in the pulse scheme depicted in Figure 1A, two product operator terms $2N_zH_z$ and N_z are present as a result of *J*-evolution during the t_1 evolution period. Assuming that cross-relaxation between H_z and N_z terms is negligible, the behavior of the $2N_zH_z$ and N_z terms during the period between points a and b is given by[20,21]

(14) Pervushin, K.; Riek, R.; Wider, G.; Wüthrich, K. *Proc. Natl. Acad. Sci. U.S.A.* **1997**, *94*, 12366−12371.
(15) Iwahara, J.; Clore, G. M. *Nature* **2006**, *440*, 1227−1230.
(16) Iwahara, J.; Zweckstetter, M.; Clore, G. M. *Proc. Natl. Acad. Sci. U.S.A.* **2006**, *103*, 15062−15067.
(17) Delaglio, F.; Grzesiek, S.; Vuister, G. W.; Zhu, G.; Pfeifer, J.; Bax, A. *J. Biomol. NMR* **1995**, *6*, 277−293.
(18) Johnson, B. A.; Blevins, R. A. *J. Biomol. NMR* **1994**, *4*, 603−614.
(19) Chance, E. M.; Curtis, A. R.; Jones, I. P.; Kirby, C. R. *FACSIMILE: a computer program for flow and chemistry simulation and general initial value problems*; Atomic Energy Research Establishment Report R8775, 1979, Harwell, H. M. Stationary Office, London.

$$\frac{\mathrm{d}}{\mathrm{d}t}\begin{pmatrix}\langle 2N_zH_z\rangle \\ \langle N_z\rangle\end{pmatrix} = -\begin{pmatrix}R_{zz} & \eta_z \\ \eta_z & R_z\end{pmatrix}\begin{pmatrix}\langle 2N_zH_z\rangle \\ \langle N_z\rangle\end{pmatrix} \quad (1)$$

where R_{zz} and R_z are relaxation rates for the $2N_zH_z$ and N_z terms, respectively, and η_z is the rate for cross-correlation between these terms. R_{zz} is significantly larger than R_z owing to $^1H-^1H$ dipolar interactions. The magnetization of each term in eq 1 is the average for the phase cycle alternating signs of *z*-magnetization, and $\langle N_z\rangle(\infty) = 0$ instead of the Boltzmann magnetization.[22] An analytical solution for eq 1 can readily be obtained using standard procedures (such as that given in ref 23):

$$\begin{pmatrix}\langle 2N_zH_z\rangle(t) \\ \langle N_z\rangle(t)\end{pmatrix} = \mathbf{P}(t)\begin{pmatrix}\langle 2N_zH_z\rangle(0) \\ \langle N_z\rangle(0)\end{pmatrix} \quad (2)$$

where the elements of $\mathbf{P}(t)$ are as follows:

$$p_{11} = \kappa \exp(-\lambda_- t) + \mu \exp(-\lambda_+ t) \quad (3)$$

$$p_{22} = \mu \exp(-\lambda_- t) + \kappa \exp(-\lambda_+ t) \quad (4)$$

$$p_{12} = p_{21} = \frac{-\eta_z}{\lambda_+ - \lambda_-}\{\exp(-\lambda_- t) - \exp(-\lambda_+ t)\} \quad (5)$$

In eqs 3−5, the rates λ_- and λ_+ are given by $\lambda_\pm = 0.5\{R_{zz} + R_z \pm \sqrt{(R_{zz} - R_z)^2 + 4\eta_z^2}\}$, and the coefficients κ and μ are given by $\kappa = 0.5\{1 - (R_{zz} - R_z)/(\lambda_+ - \lambda_-)\}$ and $\mu = 0.5\{1 + (R_{zz} - R_z)/(\lambda_+ - \lambda_-)\}$, respectively.

The simplest way to incorporate a *z*-mixing period into the TROSY-based $^1H-^{15}N$ correlation experiment is shown in Figure 1B but is problematic owing to the buildup of spurious semi-TROSY cross-peaks at (^{15}N, ^1H) = ($\Omega_N + \pi|J_{NH}|$, $\Omega_H + \pi|J_{NH}|$) arising from an imbalance in the $2N_zH_z$ and N_z terms upon increasing the mixing time *T*. Considering the phase cycle for TROSY-selection, the intensities of the TROSY cross-peak at ($\Omega_N - \pi|J_{NH}|$, $\Omega_H + \pi|J_{NH}|$) and the spurious semi-TROSY cross-peak at ($\Omega_N + \pi|J_{NH}|$, $\Omega_H + \pi|J_{NH}|$) can be calculated as a function of mixing time *T* using eqs 2−5 (Figure 2A). The simulation indicates that the two cross-peaks are of opposite sign and the signal at ($\Omega_N + \pi|J_{NH}|$, $\Omega_H + \pi|J_{NH}|$) can only be suppressed when $T = 0$ or $R_{zz} = R_z$ (which is not possible even for deuterated proteins). The buildup of the negative cross-peaks at ($\Omega_N + \pi|J_{NH}|$, $\Omega_H + \pi|J_{NH}|$) is clearly seen in the experimental spectra (Figure 2C) recorded using the pulse scheme of Figure 1B.

To solve this problem, we introduce a scheme, hereafter referred to as the S-scheme, that converts $2N_zH_z$ into $-N_z$ magnetization and N_z into $2N_zH_z$ magnetization in the middle of the *z*-mixing period and accordingly alter the phase cycle for the TROSY-selection (Figure 1A). In this case, the magnetization at the end of the *z*-mixing period (point d in Figure 1A) is given by

$$\begin{pmatrix}\langle 2N_zH_z\rangle(T) \\ \langle N_z\rangle(T)\end{pmatrix} = f\mathbf{P}\left(\frac{T}{2}\right)\mathbf{S}\mathbf{P}\left(\frac{T}{2}\right)\begin{pmatrix}\langle 2N_zH_z\rangle(0) \\ \langle N_z\rangle(0)\end{pmatrix} \quad (6)$$

$$\mathbf{S} = \begin{pmatrix}0 & 1 \\ -1 & 0\end{pmatrix} \quad (7)$$

where the coefficient *f* represents a scaling factor to account for relaxation during the S-scheme, and using eqs 3−5:

$$\mathbf{P}\left(\frac{T}{2}\right)\mathbf{S}\mathbf{P}\left(\frac{T}{2}\right) = \begin{pmatrix}0 & \exp\left(-\dfrac{R_{zz} + R_z}{2}T\right) \\ -\exp\left(-\dfrac{R_{zz} + R_z}{2}T\right) & 0\end{pmatrix} \quad (8)$$

Note that the two terms decay in a single-exponential manner with the identical relaxation rate $\bar{R} = (R_{zz} + R_z)/2$. Since an imbalance between the N_z and $2N_zH_z$ terms does not occur in this case, the semi-TROSY component does not buildup even at long *z*-mixing times *T* (Figure 2B). In addition, the process is independent of the cross-correlation rate η_z.

Next, we consider for the S-scheme the effect of slow exchange between two states *a* and *b* with rate constants k_{ab} and k_{ba} for the $a \rightarrow b$ and $b \rightarrow a$ transitions, respectively. Since the signal decays in a single-exponential manner (cf. eq 8), one would expect that the mixing time-dependence of the auto- and exchange-peaks can be described by the McConnell equations[24] for longitudinal magnetization

$$\frac{\mathrm{d}}{\mathrm{d}t}\begin{pmatrix}M^a \\ M^b\end{pmatrix} = -\begin{pmatrix}\bar{R}^a + k_{ab} & -k_{ba} \\ -k_{ab} & \bar{R}^b + k_{ba}\end{pmatrix}\begin{pmatrix}M^a \\ M^b\end{pmatrix} \quad (9)$$

where *M* represents the signal intensities of the TROSY-components. Numerical calculations indicate that this is indeed correct as shown below. Strictly speaking, the overall behavior of the *z*-magnetization terms for the two-site exchange system is given by

$$\begin{pmatrix}\langle 2H_zN_z\rangle^a(T) \\ \langle N_z\rangle^a(T) \\ \langle 2H_zN_z\rangle^b(T) \\ \langle N_z\rangle^b(T)\end{pmatrix} = f\exp\left(-\mathbf{Q}\frac{T}{2}\right)\mathbf{S}'\exp\left(-\mathbf{Q}\frac{T}{2}\right)\begin{pmatrix}\langle 2H_zN_z\rangle^a(0) \\ \langle N_z\rangle^a(0) \\ \langle 2H_zN_z\rangle^b(0) \\ \langle N_z\rangle^b(0)\end{pmatrix} \quad (10)$$

$$\mathbf{Q} = \begin{pmatrix}R_{zz}^a + k_{ab} & \eta_z^a & -k_{ba} & 0 \\ \eta_z^a & R_z^a + k_{ab} & 0 & -k_{ba} \\ -k_{ab} & 0 & R_{zz}^b + k_{ba} & \eta_z^b \\ 0 & -k_{ab} & \eta_z^b & R_z^b + k_{ba}\end{pmatrix} \quad (11)$$

$$\mathbf{S}' = \begin{pmatrix}0 & 1 & 0 & 0 \\ -1 & 0 & 0 & 0 \\ 0 & 0 & 0 & 1 \\ 0 & 0 & -1 & 0\end{pmatrix} \quad (12)$$

Figure 3 shows the time courses for the auto-peaks and exchange-peaks simulated using either eq 9 (dashed lines) or eqs 10−12 (solid lines). Although eq 9 is much simpler, the results are identical and independent of the cross-correlation rates. Thus, the S-scheme pulse sequence shown in Figure 1A permits quantitative determination of rate constants using the same calculation approach as that used for the conventional non-TROSY $^{15}N_z$-exchange experiment.

(20) Boyd, J.; Hommel, U.; Campbell, I. D. *Chem. Phys. Lett*. **1990**, *175*, 477−482.
(21) Kroenke, C. D.; Loria, J. P.; Lee, L. K.; Rance, M.; Palmer, A. G., III. *J. Am. Chem. Soc.* **1998**, *120*, 7905−7915.
(22) Sklenar, V.; Torchia, D.; Bax, A. *J. Magn. Reson*. **1987**, *73*, 375−379.
(23) Cavanagh, J.; Fairbrother, W. J.; Palmer, A. G., III; Skelton, N. J. *Protein NMR spectroscopy: Principles and Practice*; Academic Press: San Diego, CA, 1994; Chapter 5.
(24) McConnell, H. M. *J. Chem. Phys*. **1958**, *28*, 430−431.

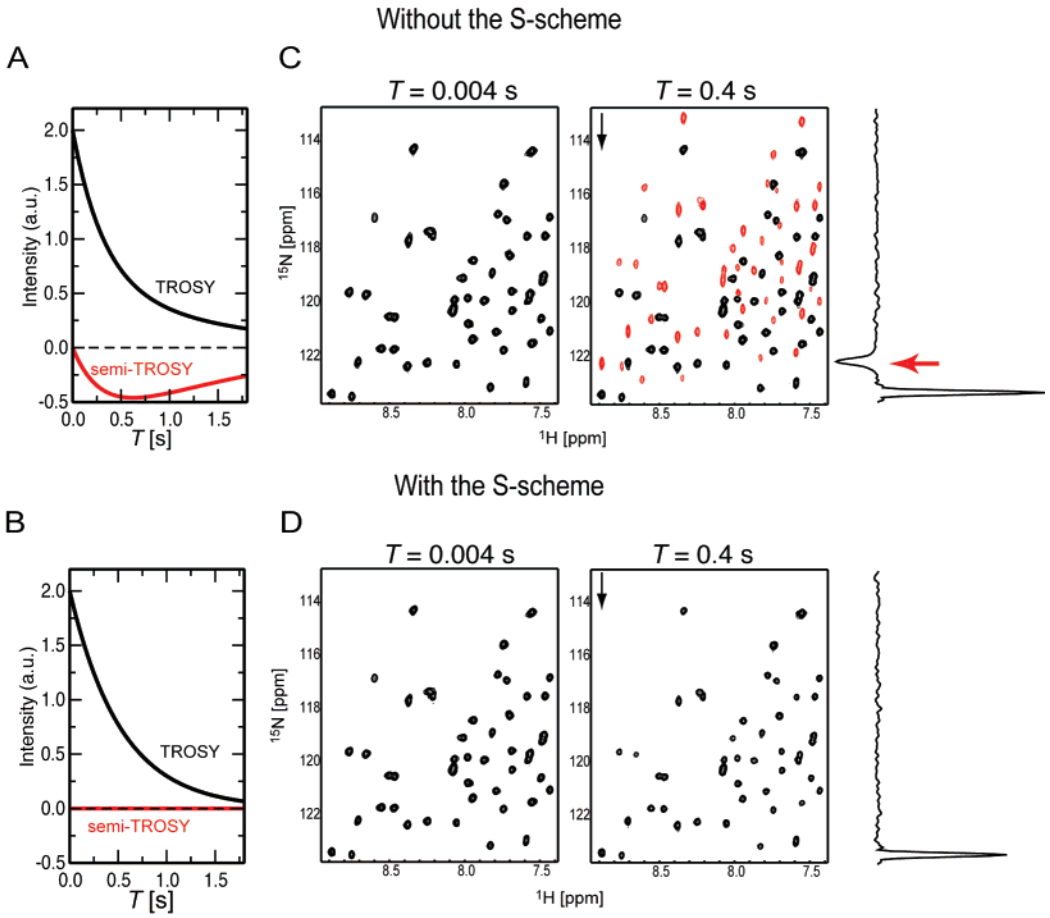

Figure 2. Suppression of spurious semi-TROSY peak buildup by the S-scheme placed in the middle of the *z*-mixing period. Simulated time courses (A) without and (B) with the S-scheme. Equations 2−5 are used for the former and eqs 6−8 are used for the latter and correspond to the pulse schemes shown in Figures 1B and A, respectively. Parameters used for these simulations were $R_{zz} = 4.8\ s^{-1}$, $R_z = 0.8\ s^{-1}$, and $\eta_z = 0.5\ s^{-1}$. The phase cycles for TROSY-selection for each experiment were taken into consideration in the simulations. Experimental TROSY-based *z*-exchange $^1H-^{15}N$ correlation spectra measured at 20 °C on the $^2H/^{15}N$-labeled HoxD9 homeodomain complexed to the 24 bp DNA duplex *a* recorded (C) without and (D) with the S-scheme using the pulse sequences shown in Figure 1B and A, respectively. Positive and negative contours are displayed in black and red, respectively. Slices along the ^{15}N-dimension of the spectrum recorded with a mixing time of $T = 0.4$ s at the positions indicated with black arrows are also shown. The appearance of spurious semi-TROSY peaks in the spectra recorded without the S-scheme is due to an imbalance between the $2H_zN_z$ and N_z terms arising from their different relaxation rates.

Results and Discussion

We used the TROSY-based *z*-exchange experiment to study the temperature dependence of the kinetics of translocation of the homeodomain transcription factor HoxD9 from a specific target site on one DNA molecule to the specific target site on another DNA molecule using the "mixture approach" employed in our previous studies.[11,15,16] In this approach three macromolecular components are mixed together: $^2H/^{15}N$-labeled HoxD9 homeodomain and two 24-bp DNA duplexes *a* and *b* (Figure 4A). The two DNA duplexes *a* and *b* are identical except for a single base pair mutation immediately adjacent to the central six base-pair specific target site and the affinities of HoxD9 for the two duplexes are virtually identical.[11] For some residues, the chemical shifts of the $^1H-^{15}N$ correlation cross-peaks arising from the two complexes are slightly different owing to the difference in DNA sequence, thereby permitting us to study the kinetics of the exchange reaction in which the homeodomain is transferred from one DNA molecule to another. Previous studies have shown that at high concentrations of free DNA ($>10^{-6}$ M) intermolecular translocation of the HoxD9 homeodomain takes place predominantly through a direct transfer mechanism rather than via a two-step mechanism involving dissociation of the protein into free solution followed by reassociation.[11] Direct transfer, also known as "intersegment transfer", is a second-order reaction in which collision between the protein−DNA complex and free DNA mediates intermolecular translocation.[25−29] As described previously,[11] the behavior of longitudinal components of the magnetization for the direct transfer process can be described by eq 9, in which the apparent translocation rate is given by the product of the second-order rate constant for direct transfer and the concentration of free DNA. Under the present experimental conditions, translocation of HoxD9 between the two DNA duplexes *a* and *b* is in the slow exchange regime. Figure 4B shows the autopeaks and exchange peaks arising from the backbone amide group of Arg-5 at 20 °C at

(25) Berg, O. G.; Winter, R. B.; von Hippel, P. H. *Biochemistry* **1981**, *20*, 3040−3052.
(26) Fried, M. G.; Crothers, D. M. *J. Mol. Biol.* **1984**, *172*, 263−282.
(27) Ruusala, T.; Crothers, D. M. *Proc. Natl. Acad. Sci. U.S.A.* **1992**, *89*, 4903−4907.
(28) Cho, S.; Wensink, P. C. *J. Biol. Chem.* **1997**, *272*, 3185−3189.
(29) Lieberman, B. A.; Nordeen, S. K. *J. Biol. Chem.* **1997**, *272*, 1061−1068.
(30) Hovde, S.; Abate-Shen, C.; Geiger, J. H. *Biochemistry* **2001**, *40*, 12013−12021.
(31) Fraenkel, E.; Pabo, C. O. *Nat. Struct. Biol.* **1998**, *5*, 692−697.

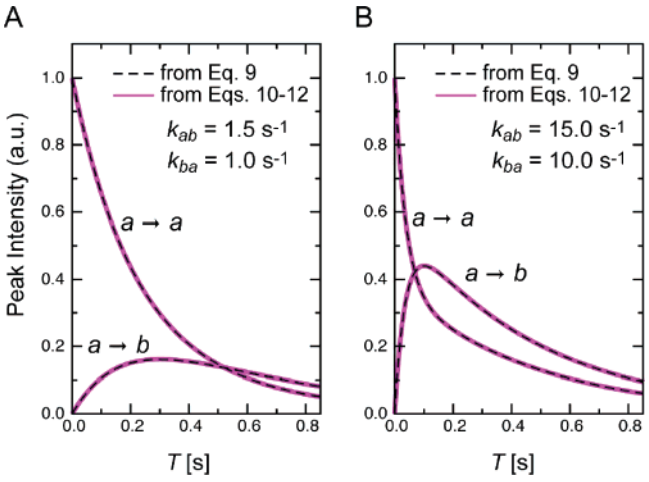

Figure 3. Simulations of time courses of auto- and exchange-peak intensities for the TROSY-based *z*-exchange experiment with the S-scheme. Two panels show results of simulations employing a different set of kinetic rate constants (A, $k_{ab} = 1.5$ s^{-1} and $k_{ba} = 1.0$ s^{-1}; B, $k_{ab} = 15.0$ s^{-1} and $k_{ba} = 10.0$ s^{-1}). The other parameters employed in each calculation are as follows: $R^a_{zz} = 4.8$ s^{-1}, $R^a_z = 0.8$ s^{-1}, $\eta^a_z = 0.5$ s^{-1}, $R^b_{zz} = 3.0$ s^{-1}, $R^b_z = 0.5$ s^{-1}, and $\eta^b_z = 0.3$ s^{-1}. The solid magenta lines are calculated with eqs 10−12 for ($a \rightarrow a$) auto- and ($a \rightarrow b$) exchange-peaks, whereas the dotted black lines are obtained using eq 9. For all examined values of the parameters R_{zz}, R_z, η_z, k_{ab}, and k_{ba}, the results from eqs 10−12 were found to be identical with those with eq 9. Thus rate constants can be obtained in the same way as that for the conventional non-TROSY *z*-exchange experiment.

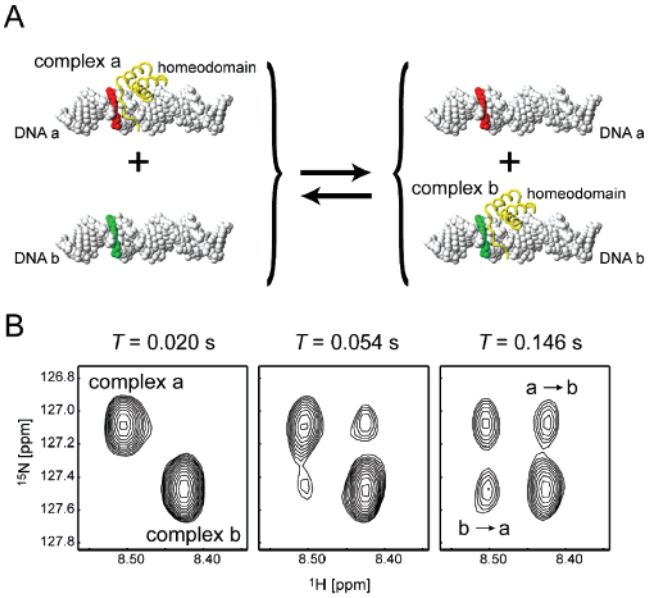

Figure 4. Intermolecular translocation of HoxD9 between specific sites located on different DNA duplexes. (A) The system studied: the NMR sample contains three macromolecular components: the ^{2}H/^{15}N-labeled HOXD9 homeodomain and two 24-bp DNA duplexes *a* and *b*. Red (C·G) and green (A·T) represent the base pair at position 8 that is different between DNA duplexes *a* and *b*. (B) Auto- and exchange-peaks arising from the backbone amide group of Arg-5 observed in the TROSY-based *z*-exchange experiment recorded with three different mixing times *T*. The spectra were obtained at 20 °C.

three mixing times (20, 54, and 146 ms) using the TROSY-based *z*-exchange ^{1}H−^{15}N correlation experiment. The exchange peaks are apparent in the spectra recorded with the two longer mixing times. Using data collected at eight different mixing times, we were able to determine the translocation rates by nonlinear least-squares fitting to the experimental time dependence of the exchange- and auto-peak intensities.

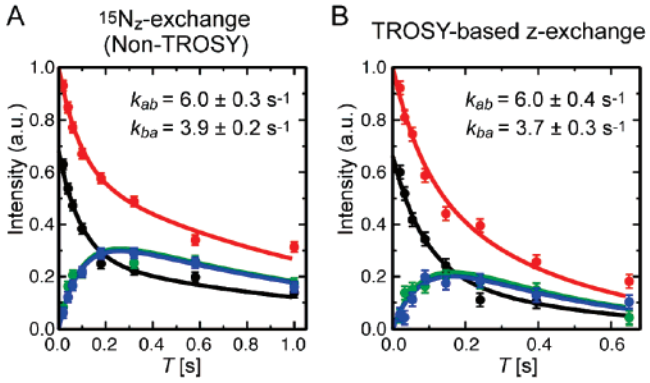

Figure 5. Comparison of (A) the conventional non-TROSY ^{15}N$_z$-exchange experiment[5] and (B) the present TROSY-based *z*-exchange experiment for quantitative evaluation of rate constants. The experimental intensities for the auto- and exchange-peaks of Arg-5 (20 °C) as a function of mixing time together with the best-fit theoretical curves obtained by nonlinear least-squares optimization are shown (black, a → a; red, b → b; green, a → b; blue, b → a). The values of k_{ab} and k_{ba} obtained are displayed in the figures and are identical within experimental error for the two experiments. The longitudinal relaxation rates for complexes *a* and *b* were assumed to be identical. The values of the relaxation rates were calculated to be $\bar{R} = 2.8$ s^{-1} for the TROSY-based *z*-exchange experiment and $R_z = 0.8$ s^{-1} for the conventional non-TROSY ^{15}N$_z$-exchange experiment.

Comparison of TROSY-Based and Non-TROSY N$_z$-Exchange Experiments. Data on the same sample were collected at 20 °C using the conventional non-TROSY ^{15}N$_z$ exchange experiment[5] to compare the reliability of the rate constants derived from the non-TROSY and TROSY-based pulse sequences. As is evident from Figure 5, the time courses for the autopeak and exchange peak intensities observed for the two experiments appear to be quite different. This is simply due to the fact that the apparent longitudinal relaxation rate during the mixing period is faster for the TROSY-based *z*-exchange experiment due to the 50% contribution from R_{zz} (see eq 8). However, the protein translocation rates, k_{ab} and k_{ba}, determined by least-squares analysis using eq 9 are identical within experimental error for the two experiments (Figure 5). This observation provides experimental confirmation that the TROSY-based and conventional non-TROSY *z*-exchange experiments can be analyzed in the same way.

The line shapes of the auto- and exchange-peaks in the TROSY-based *z*-exchange ^{1}H−^{15}N correlation experiment are significantly narrower than those in the ^{15}N$_z$-exchange experiment, which is especially advantageous at low temperature and high magnetic field. This is clearly illustrated in Figure 6 which provides a comparison of the two experiments for the auto- and exchange-peaks of the backbone amide group of Thr-9 measured at 8 °C and a ^{1}H-frequency of 800 MHz (with a mixing time of 0.38 s). In the case of Thr-9 the ^{1}H- and ^{15}N-chemical shift differences between complexes *a* and *b* are relatively small. As a result the auto- and exchange-peaks of Thr-9 are not resolved in the conventional non-TROSY ^{15}N$_z$-exchange (Figure 6A) but are clearly resolved in the TROSY-based *z*-exchange experiment due to the better line shapes (Figure 6B). Thus, the TROSY-based *z*-exchange experiment is useful for kinetic analysis either at low temperature and/or for a large molecular weight systems.

Determination of the Activation Energy for Intermolecular Translocation of HoxD9 between Specific Sites on Different DNA Molecules. Using the TROSY-based *z*-exchange experiment, we measured the translocation rates at 8, 15, 20, 30, and 35 °C. The translocation rates at 8 °C were ∼15-fold

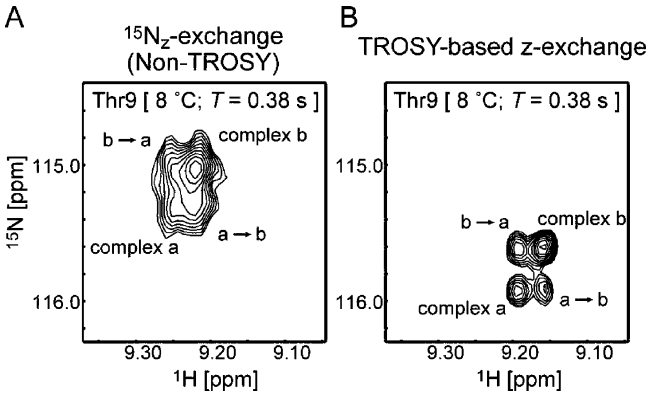

Figure 6. The TROSY-principle improves separation of auto- and exchange-peaks at low temperature. Signals from Thr-9 obtained at 8 °C (A) with the conventional non-TROSY $^{15}N_z$-exchange experiment[5] and (B) with the TROSY-based *z*-exchange experiment (Figure 1A) using the same mixing time (T = 0.38 s) are displayed. Data were measured using the same digital resolution and processed in an identical manner.

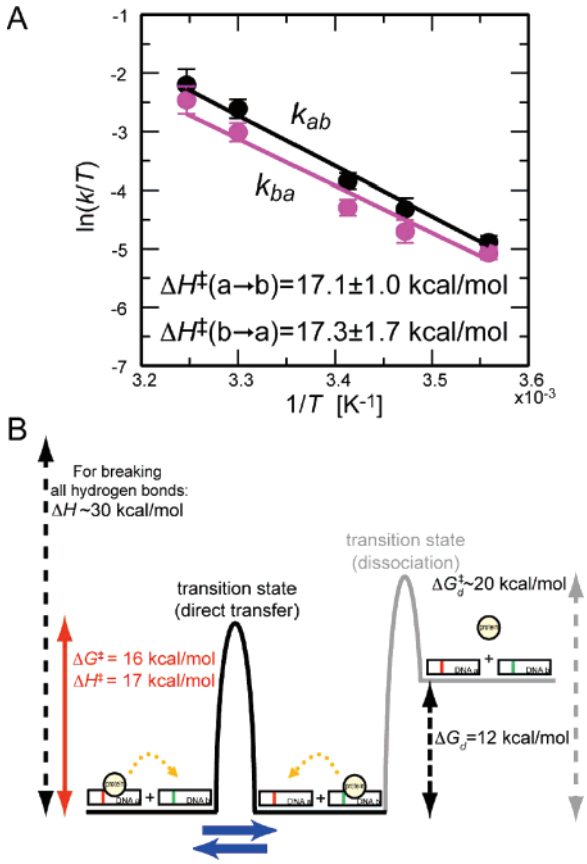

Figure 7. Energetics of translocation of HoxD9 between specific sites on different DNA molecules. (A) Eyring plots of the translocation rates measured at 8, 15, 20, 30, and 35 °C (k_{ab}, black; k_{ba}, magenta). The activation enthalpy ($\Delta H^{\ddagger}$) and entropy ($\Delta S^{\ddagger}$) were determined using the Eyring equation (see text). (B) Schematic diagram comparing the energetics of translocation (red) and dissociation (see text). Blue arrows represent the intermolecular translocation process characterized in the present study. The enthalpy for breaking all intermolecular hydrogen bonds (~30 kcal/mol) was estimated from the crystal structures of two highly homologous homeodomain−DNA complexes (PDB codes 1IG7[30] and 9ANT[31]).

slower than those at 35 °C. Figure 7A shows Eyring plots of the temperature-dependence of the translocation rates k_{ab} and k_{ba}. The activation enthalpy ($\Delta H^{\ddagger}$) and entropy ($\Delta S^{\ddagger}$) were determined using the Eyring equation ($\ln k/T = -\Delta H^{\ddagger}/RT + \ln k_B/h + \Delta S^{\ddagger}/R$, where k_B is the Boltzmann constant, h, Planck's constant, and R, the gas constant). The obtained values were $\Delta H^{\ddagger} = 17.1 \pm 1.0$ kcal·mol^{-1} and $\Delta S^{\ddagger} = 3.7 \pm 3.4$ cal·mol^{-1}·K^{-1} for the translocation from DNA *a* to *b*; $\Delta H^{\ddagger} = 17.3 \pm 1.6$ kcal·mol^{-1} and $\Delta S^{\ddagger} = 3.9 \pm 5.6$ cal·mol^{-1}·K^{-1} for *b* to *a*. Since activation free energies at 298 K ($\Delta G^{\ddagger}_{298K}$) are calculated to be 16 kcal·mol^{-1}, the energy barrier for protein translocation between DNA molecules is primarily enthalpic in origin.

It is interesting to compare the energetics of translocation with those for the dissociation process from the bound state to the free state. The free energy difference between the two states (ΔG_d) can be calculated from the equilibrium dissociation constant. For the specific interaction between the HoxD9 homeodomain and the 24-bp DNA duplexes containing the specific target sequence, ΔG_d at 298 K is calculated to be 12 kcal/mol. The rate constant k_{off} for dissociation of HoxD9 from its specific DNA site, determined from gel shift assays, is 0.01 s^{-1}.[32] From this value and the equation $k_{off} = (k_B T/h) \exp\{-\Delta G^{\ddagger}_d/(RT)\}$, the activation free energy for the dissociation process ($\Delta G^{\ddagger}_d$) is estimated to be 20 kcal/mol. Thus, the energy barrier for translocation through the direct transfer mechanism[11] is significantly lower than that for dissociation. A schematic comparison of the energetics of translocation and dissociation is shown in Figure 7B.

Concluding Remarks

In this paper, we have presented TROSY-based *z*-exchange spectroscopy for quantitative measurement of rate constants for a system in the slow exchange regime. During the preparation of the present manuscript, Peruvshin et al.[33] published a pseudo-four-dimensional TROSY-based spin-state exchange experiment that is quite different from ours. These experiments were designed for assignment purposes rather than for quantitative use to measure rate constants. (Indeed, Peruvshin et al. made use of a conventional *zz*-exchange experiment to determine the exchange rate in their system.) Our TROSY-based *z*-exchange experiment presented here permits quantitative determination of rate constants in the same manner as that employed for conventional non-TROSY exchange experiments. Because of the use of the TROSY principle, kinetic measurements are feasible over a wider range of temperatures and for larger molecular weight systems than was heretofore possible, thereby making feasible analysis of activation energies for biologically important processes involving macromolecules.

Acknowledgment. This work was supported by startup funds from the University of Texas Medical Branch (to J.I.) and by the Intramural Program of the National Institute of Diabetes and Digestive and Kidney Diseases, National Institutes of Health (to G.M.C.). We thank Dr. Shanmin Zhang for supporting the NMR instruments at UTMB.

Note Added after ASAP Publication: On October 18, 2007, a production error in an equation on the third page was corrected.

JA074604F

(32) Catron, K. M.; Iler, N.; Abate, C. *Mol. Cell Biol*. **1993**, *13*, 2354−2365.
(33) Nikolaev, Y.; Pervushin, K. *J. Am. Chem. Soc*. **2006**, *129*, 6461−6469.
(34) Levitt, M. H. *J. Magn. Reson*. **1997**, *126*, 164−182.
(35) Rance, M.; Loria, J. P.; Palmer, A. G., III. *J. Magn. Reson*. **1999**, *136*, 92−101.
(36) Schulte-Herbrüggen, T.; Sørensen, O. W. *J. Magn. Reson*. **2000**, *144*, 123−128.
(37) Güntert, P.; Schaefer, N.; Otting, G.; Wüthrich, K. *J. Magn. Reson., Ser. A* **1993**, *101*, 103−105.